relative expression level of each uptake transporter in *Xenopus* oocytes is similar to that in rat liver. This approach has also been applied to human sandwich-cultured hepatocytes in a study (Liao et al. 2010) that found that the expression of uptake transporters did not change much in human sandwich-cultured hepatocytes, but decreased rapidly with time in rat sandwich-cultured hepatocytes (Kotani et al. 2011). A recent report showed that the relative contributions of OATP1B1 to the uptake of several substrates estimated with OATP1B1 siRNA were similar to those obtained from RAF methods (Williamson et al. 2013).

Regarding the biliary efflux transporters, Tian et al. succeeded in the application of siRNAs targeted to Mrp2 and Mrp3 in sandwich-cultured rat hepatocytes (Tian et al. 2004). The knockdown of Mrp2 resulted in a decrease in the biliary excretion index (BEI) of carboxy dichlorofluorescein (CDF), whereas knockdown of Mrp3 caused an increase in BEI; the extent of the decrease in protein expression was similar to the change in CDF uptake. Yue et al. also established an adenoviral vector expressing Bcrp siRNA; its infection into rat sandwich-cultured hepatocytes led to a decrease in the BEI for nitrofurantoin, a typical substrate of Bcrp, but not for digoxin, a typical P-gp substrate (Yue et al. 2009).

6.3.3 *Determination of the Intrinsic Clearance of Each Transport Process of a Substrate*

As mentioned in Sect. 6.2.2, overall intrinsic clearance is determined by several intrinsic processes; thus, the intrinsic clearance of uptake, backflux, biliary excretion, and metabolism of a substrate should be determined separately in the accurate prediction of DDIs. Hepatic uptake intrinsic clearance can be determined by an uptake assay with isolated hepatocytes. As is often the case with transporter substrates, if the uptake is the rate-determining process in the overall intrinsic hepatic clearance, the uptake intrinsic clearance can approximate the intrinsic hepatic clearance. Watanabe et al. demonstrated that the predicted hepatic clearances of several transporter substrates obtained from in vitro uptake assays with rat isolated hepatocytes correlated strongly with their observed biliary excretion clearances in rats (Watanabe et al. 2009a). The intrinsic hepatic clearance calculated from nonrenal clearance of compounds was also predicted well in humans from in vitro uptake assays with human cryopreserved hepatocytes (Watanabe et al. 2011). Soars et al. reported that the initial disappearance rates of parent compounds from the incubation buffer ("media-loss assay") predicted the in vivo intrinsic clearances better than did their clearances calculated from the AUCs of the parent compounds in the whole suspension, suggesting that hepatic uptake clearance mainly determines the overall hepatic intrinsic clearance and that the β value is thought to be nearly equal to 1 for these compounds (Soars et al. 2007).

The intrinsic clearance for each process can be determined by several methods. One approach is to evaluate each intrinsic clearance separately with different experimental systems and some assumptions. Watanabe et al. evaluated the uptake intrinsic clearance from uptake assays with isolated human hepatocytes. They used an empirical scaling factor calculated from the ratio of in vivo uptake clearance to in vitro uptake clearance in rats, the sinusoidal efflux clearance from the nonsaturable uptake intrinsic clearance, biliary excretion clearance from transport in rat CMVs, and metabolic clearance from the S9 fraction to predict the whole-body pharmacokinetics of pravastatin in humans (Watanabe et al. 2009b). Umehara et al. determined the uptake clearance in isolated rat hepatocytes, sinusoidal efflux clearance, and biliary excretion clearance in sandwich-cultured rat hepatocytes, and metabolic clearance in rat microsomes for 13 compounds (Umehara and Camenisch 2012). They succeeded in finding a good prediction of in vivo hepatic clearances from the predicted clearances calculated based on (6.8) with in vitro parameters.

Another approach is to fit the in vitro time profile of the uptake of compounds in human hepatocytes to a mechanistic compartmental model that considers multiple intrinsic processes to determine simultaneously several intrinsic clearances from a single experimental system. Menochet et al. determined the kinetic parameters for uptake, sinusoidal efflux (considering only nonsaturable diffusion), and metabolism of repaglinide and telmisartan at the same time by fitting their time- and concentration-dependent uptake in human short-term (2 h) cultured rat hepatocytes to an extended mechanistic two-compartment model that included saturable and nonsaturable uptake clearance, sinusoidal efflux clearance, and metabolic clearance (Menochet et al. 2012). Jones et al. determined the multiple intrinsic clearances of uptake, sinusoidal efflux, and biliary excretion of various OATP substrates by the fitting their time profiles of uptake into sandwich-cultured human hepatocytes to a mechanistic two-compartment model including uptake, sinusoidal efflux, and biliary excretion (Jones et al. 2012). However, further empirical scaling factors are needed for the accurate prediction of pharmacokinetics of multiple drugs.

6.3.4 *Estimation of the $K_{p,uu}$ Value of an Inhibitor in Hepatocytes*

As discussed above, when considering the inhibition of intracellular targets such as metabolic enzymes and efflux transporters, the intracellular unbound concentration of inhibitor should be estimated for the accurate DDI prediction. It is impossible to measure the unbound intracellular concentration of inhibitor drugs in humans, and appropriate in vitro methods to estimate the $K_{p,uu}$ value are needed. The $K_{p,uu}$ value is theoretically described as follows (Shitara et al. 2013):

$$K_{p,uu} = \frac{PS_{inf,act} + PS_{dif}}{PS_{dif} + PS_{ex} + CL_{int}} \tag{6.25}$$

$PS_{inf,act}$, PS_{dif}, PS_{ex}, and CL_{int} represent the intrinsic clearances for active influx transport, diffusional membrane transport, biliary efflux transport, and metabolism, respectively, assuming that sinusoidal efflux comprises only passive diffusion.

A traditional uptake study with hepatocytes can measure only the uptake amount of total (unbound+bound) compounds. Thus, some appropriate methods to estimate separately the unbound intracellular concentration of compounds in hepatocytes are needed. Yabe et al. reported $K_{p,uu}$ values of anionic compounds determined by using the results of an in vitro uptake assay in human hepatocytes with a nonspecific CYP inhibitor and calculated by the following equation (Yabe et al. 2011):

$$K_{p,uu} = 1 + \frac{V_{max,inf} / K_{m,inf}}{PS_{dif}} \tag{6.26}$$

$V_{max,inf}$ and $K_{m,inf}$ represent the maximum transport rate and Michaelis–Menten constant for active influx transport, respectively. The $K_{p,uu}$ value calculated by (6.26) may include the membrane transport by facilitated diffusion and active transport, and this method does not consider the metabolic intrinsic clearance, which results in the overestimation of the true $K_{p,uu}$ value. Another strategy to estimate the $K_{p,uu}$ value is to stop the active transport without changing any processes (passive diffusion, intracellular binding, etc.). For this purpose, several strategies can be proposed including (1) decreasing the temperature (on ice), (2) adding a potent inhibitor of uptake transporters (e.g., rifampicin for anionic compounds), or (3) using high concentrations of substrates to saturate the uptake transporters. Application of ATP depletors is theoretically possible, but previous studies suggested that moderate concentrations of ATP depletors, which did not cause cell toxicity, could not completely inhibit the function of active transport. Although in vitro uptake experiments with isolated hepatocytes are easy, previous reports indicated that isolated hepatocytes lose their cell polarity and the functions of biliary efflux transporters decrease, thus the predicted $K_{p,uu}$ value may overestimate the real value. By contrast, sandwich-cultured hepatocytes can reproduce all the transport and metabolic functions of hepatocytes and is suitable for the estimation of the $K_{p,uu}$ value. However, we note that expression/function of some transporters and metabolic enzymes decrease rapidly with culture time, especially in cultures of rodent cells (Ishigami et al. 1995; Jigorel et al. 2005; Rippin et al. 2001; Kotani et al. 2011). Further validation of the methods is needed.

6.4 Quantitative Prediction of the Risk of TP-DDIs in the Liver

6.4.1 *Prediction Strategies of TP-DDIs: A Static Model and Dynamic Model*

The I_u value is essential for estimating the inhibition potency of inhibitors (R value), thus the precise estimation of the I_u value should be needed for the accurate prediction of DDIs. Considering the definition of I_u, which is the protein-unbound concentration of an inhibitor in the vicinity of a target transporter, one must estimate the unbound inhibitor concentration in the blood facing the hepatocytes when determining DDIs involving hepatic uptake transporters. By contrast, for DDIs involving hepatic efflux transporters, one must estimate the unbound inhibitor concentration in the hepatocytes. However, it is difficult to estimate the I_u value accurately in humans because it cannot be directly measured. In addition, in a real situation, the I_u value always changes over time. To predict accurately the ratio of plasma AUC in the presence of inhibitor drugs to that in their absence (AUCR; $AUC_{+inhibitor}/AUC_{control}$), the time profiles of plasma and tissue concentrations of both the substrate and inhibitor drugs need to be reproduced. One possible approach is to construct an appropriate mathematical model to explain the real-time whole-body disposition of drugs. This approach is referred to as a "dynamic model" in the US FDA draft guidance (US Food and Drug Administration (FDA) 2012). The physiologically based pharmacokinetic (PBPK) model comprises multiple compartments corresponding to the tissues and blood pool, which are connected by blood flow to mimic the blood circulation in the body. Thus, the PBPK model enables one to observe the itinerary of a drug inside the body after its administration simply by in silico simulation. However, it is essential, but difficult, to set up the kinetic parameters in such a model because only the time profiles of the plasma concentration and urinary excretion of drugs can be obtained from humans, and multiple sets of parameters may be able to apparently reproduce the limited clinical data.

In vitro experimental data can be used to provide a clue to the optimized model parameters; good methods for in vitro–in vivo scale-up have been proposed by several researchers, but their universality has not been confirmed yet (Barton et al. 2013; Houston et al. 2012; Zamek-Gliszczynski et al. 2013). Particularly in the early stage of drug development, the pharmacokinetic properties of drug candidates in humans have not been well characterized in humans, and it is difficult to apply a dynamic model approach to DDI prediction. Instead, assuming that the inhibitor concentration is maintained at the same level, one can simply calculate the R value and subsequent AUC changes for substrates if one can identify an appropriate I_u value. This approach is referred to as the "static model" in the US FDA draft guidance (US Food and Drug Administration (FDA) 2012). To avoid false-negative predictions (clinically significant DDIs cannot be forecasted by the DDI prediction method), the I_u value can be set as a constant at the theoretical maximum concentration at the target site. Recent progress for this detailed prediction method is discussed below.

6.4.2 *Prediction of TP-DDIs in the Liver with a Static Model*

In the prediction of the risk of transporter-mediated DDIs with a static model, one key factor is to determine what kind of inhibitor drug concentration should be used to estimate the inhibition potencies of transporters in the liver. According to the traditional pharmacokinetic theory, the inhibitor concentration must be defined as that at the vicinity of the transporters, and only the protein-unbound form of

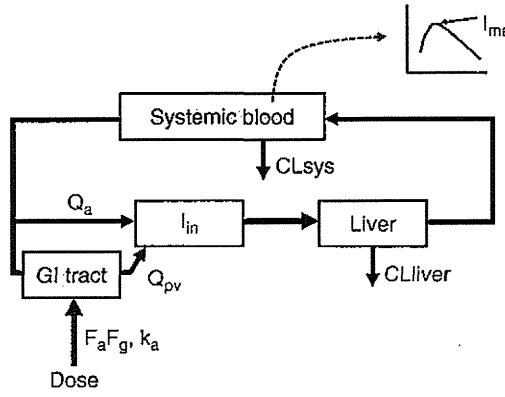

Fig. 6.4 Mathematical model for estimating $I_{u,in,max}$ value of inhibitors (cited from Ito et al. 1998)

inhibitors can be involved in the inhibition of transporter function. Thus, the unbound blood concentration of inhibitors on the basal side of hepatocytes must be used for the prediction of inhibition potency against hepatic uptake transporters, whereas the unbound concentration in the hepatocytes must be used against hepatic efflux transporters. A static model is often applied for the sensitive detection of the signal of DDI risk, especially in the early stage of drug development when the detailed pharmacokinetic properties of a newly developed drug have not been well characterized in humans. Thus, it is essential to avoid the false-negative prediction, in which significant DDI actually occurs in the clinical situation, even though the DDI risk has been predicted to be negative. However, we also need to reduce the number of false-positive predictions because the number of DDI-positive cases increases as the inhibitor concentrations used for DDI prediction increase. Thus, one rational solution for this issue is to use the theoretically achievable maximum unbound concentration of inhibitors at the target site without considering their unrealistically excessive concentrations.

In the field of CYP-mediated metabolism, Ito et al. proposed a method to calculate the theoretically maximum unbound concentration of inhibitors at the inlet to the liver (Ito et al. 1998). The mathematical model for considering this method is shown in Fig. 6.4. For orally administered inhibitor drugs, the drugs flowing into the liver comprise those from the circulating blood supplied via the hepatic artery and those absorbed from the intestine supplied via the portal vein. Thus, it is possible that the inhibitor concentration is higher at the inlet to the liver than in the systemic blood. Based on this model, the amount (X_{abs}) and velocity (v_{abs}) of the drugs absorbed from the intestine into the portal vein can be described by the following equations:

$$X_{abs} = F_a F_g \text{ Dose } \left(1 - e^{-k_a t}\right) \tag{6.27}$$

$$v_{abs} = \frac{dX_{abs}}{dt} = k_a \ F_a F_g \text{ Dose } e^{-k_a t} \tag{6.28}$$

F_aF_g, k_a, and t represent the intestinal availability (fraction of drugs absorbed into the portal vein from the intestinal lumen), absorption rate constant, and time after oral administration, respectively. Thus, the flow rate of a drug into the liver (v_{in}) is calculated as follows:

$$v_{in} = Q_a \ I + Q_{pv} \ I + k_a \ F_a F_g \text{ Dose } e^{-k_a t} \tag{6.29}$$

Q_a, Q_{pv}, and I represent the blood flow rate at the hepatic artery, blood flow rate at the portal vein, and the concentration of inhibitors in the circulating blood. When considering the maximum v_{in} value based on (6.29), the observed maximum inhibitor concentration in the blood (I_{max}) can be used as the I value, and t should be 0 to maximize the v_{abs} value. Therefore, considering that the hepatic blood flow rate (Q_h) is the sum of Q_a and Q_{pv}, the protein-unbound maximum inhibitor concentration at the inlet to the liver ($I_{u,in,max}$) can be described as indicated in (6.30).

$$I_{u,in,max} = f_B \frac{v_{in}}{Q_h} = f_B \left(I_{max} + \frac{k_a \ F_a F_g \text{ Dose}}{Q_h} \right) \tag{6.30}$$

f_B indicates the protein-unbound fraction in blood. Because the F_aF_g and k_a values are not obtained easily, especially in the early stage of drug development, these values must be set as 1 and 0.1 min^{-1} (maximum gastric emptying time), respectively, because the maximum inhibitor concentration must be estimated for this calculation. When interpreting the results obtained from this approach, one should keep in mind that if the calculated R value ($=1+I/K_i$) with $I_{u,in,max}$ is close to 1, one can neglect the risk of DDIs, whereas even if the R value is estimated to be more than 1, one can never say that DDIs could occur in the clinical situation because the $I_{u,in,max}$ value always overestimates the real inhibitor concentration. This method is useful for sensitively screening out the possible DDI cases but is not suitable for the accurate prediction of the extent of the change in the AUC by DDIs; instead, prediction with a dynamic model should be considered for such purpose.

Ito et al. demonstrated the effectiveness of the prediction of DDI risk mediated by CYP enzymes using $I_{u,in,max}$ values (Ito et al. 2002). They analyzed the literature for CYP-mediated DDI cases and showed that the number of false-negative predictions was best minimized by the use of $I_{u,in,max}$ values rather than the unbound concentration of inhibitors in the blood ($I_{u,max}$) or total (bound+unbound) concentration of inhibitors in the blood (I_{max}) and that the number of true positive predictions was also highest using $I_{u,in,max}$ values. As shown for OATP transporters, Hirano et al. and Matsushima et al. investigated the inhibitory effects of several inhibitor drugs on the OATP1B1-mediated pitavastatin uptake and OATP1B3-mediated fexofenadine uptake in transporter-expressing HEK293 cells (Hirano et al. 2006; Matsushima et al. 2008). In their analyses, drugs with estimated R values at a therapeutic dose of more than two include cyclosporine A, rifampicin, rifamycin SV, clarithromycin, indinavir, and ritonavir for OATP1B1, and cyclosporine A and rifampicin for

OATP1B3. For most of these drugs, clinical DDI cases have also been reported, suggesting the validity of this prediction using a static model with $I_{u,in,max}$ value. Examples of the results calculated for marketed drugs using a static model with $I_{u,in,max}$ values are summarized in Table 6.1. This table shows that even if the K_i values of drugs for OATP transporters are relatively small, clinically relevant DDIs should not be seen in most cases in a static model prediction with $I_{u,in,max}$ values because of the low clinical dose and extensive protein binding of drugs. OATP1B1 can transport drugs and bilirubin, the breakdown product of normal heme catabolism (Cui et al. 2001). Thus, the potent inhibition of OATP1B1 by drugs results in the decreased hepatic clearance of bilirubin and subsequent drug-induced hyperbilirubinemia. Campbell et al. examined the inhibitory effects of several drugs on the OATP1B1-mediated uptake of $E_2$17βG to screen out the drugs that can induce hyperbilirubinemia (Campbell et al. 2004). Even though they used the $I_{u,max}$ value, which should be lower than $I_{u,in,max}$, when calculating their R values, indinavir, cyclosporine A, and rifamycin SV were estimated to inhibit OATP1B1-mediated transport by 41 %, 43 %, and 96 %, respectively. This is in good agreement with the clinical reports in which indinavir and cyclosporine A caused unconjugated hyperbilirubinemia in some, but not all, human subjects, whereas rifamycin SV caused hyperbilirubinemia in all subjects. By contrast, saquinavir inhibited OATP1B1 function by only 7 % in their estimation, which is also supported by a clinical report showing that saquinavir is not known to cause hyperbilirubinemia. Thus, the method for DDI prediction with a static model may also be used for the detection of the risk of drug-induced hyperbilirubinemia in the early stage of drug development.

Yoshida et al. recently investigated the predictability of the risk of DDIs involving OATP transporters using a static model (Yoshida et al. 2012). They systematically collected the 58 DDI studies involving 12 substrates of OATP transporters from the literature. They estimated the R value for each case and compared the predicted AUC increases with those observed and evaluated the effects of three assumptions on the number of false-negative predictions. In the first assumption, the maximum inhibitory effects of CYP3A and efflux transporters (P-gp, MRP2, BCRP) were considered if they were judged to be inhibited by drugs in the small intestine when using the drug interaction number (DIN) proposed by Tachibana et al. (2009). They defined DIN as the dose divided by the K_i value and set up the threshold values as 2.8 L for CYP3A and 10.8 L for P-gp, above which inhibition of CYP3A or P-gp may occur in the human intestine. Thus, if the DINs of inhibitor drugs exceeded the threshold values, F_aF_g values were assumed to be 1 when inhibitor drugs were coadministered. When evaluating the impact of this assumption, the number of false-negative predictions was decreased slightly from 19 to 16 studies with this assumption for F_aF_g values.

In the second assumption, Tachibana et al. compared the number of false-negative predictions when an inhibitor concentration was set to the following three choices: theoretically maximum unbound concentration at the inlet to the liver ($I_{u,in,max}$) (calculated from (6.30)), maximum unbound concentration in the blood circulation ($I_{u,max}$), and maximum total (unbound+bound) concentration in the blood circulation (I_{max}) (Fig. 6.5). As expected from the previous results of a static prediction of

Table 6.1 Inhibitory effects of selected drugs on the transport function of OATP1B1 and OATP1B3

Pharmacological action	Name	K_i or IC_{50} value for OATP1B1 (μM)	K_i or IC_{50} value for OATP1B3 (μM)	Dose (mg)	f_B	$I_{u,max}$ (μM)	$I_{u,in,max}$ (μM)	*R* value for OATP1B1	*R* value for OATP1B3
HIV protease inhibitors	Amprenavir	13	13	700	0.1	0.69	7.7	1.6	1.6
	Atazanavir	1.8	2.0	300	0.096	0.83	3.6	**3.0**	**2.8**
	Darunavir	3.1	3.3	600	0.05	0.54	4.0	**2.3**	**2.2**
	Lopinavir	0.50	5.1	400	0.015	0.23	0.89	**2.8**	1.2
	Nelfinavir	0.93	–	750	0.01	0.086	0.91	**2.0**	–
	Ritonavir	1.0	3.8	800	0.02	0.57	2.1	**3.1**	1.6
	Saquinavir	1.8	2.8	400	0.02	0.087	0.91	1.5	1.3
	Tipranavir	1.1	3.2	500	0.0042[a]	1.2	1.8	**2.6**	1.6
Macrolides	Clarithromycin	28	54	400	0.54	1.0	21	1.8	1.4
	Erythromycin	11	38	200	0.36	0.4	6.5	1.6	1.2
	Telithromycin	120	11	800	0.47	0.65	33	1.3	**4.0**
Immunosuppressants	Cyclosporin A	0.15	0.68	200	0.1	0.18	1.3	**9.7**	**2.9**
	Tacrolimus	0.61	–	9.6	0.01	0.00055	0.0080	1.0	–
Fibrates	Bezafibrate	45	–	200	0.06	0.58	2.6	1.1	–
	Fenofibrate	110	–	106.6	0.01	0.25	0.43	1.0	–
	Gemfibrozil	20	10	600	0.0065[a]	1.5	3.2	1.2	1.3
	(GEM-glu)[b]	14	74	–	0.12	2.3	–	1.2	1.0
Antidiabetic drugs	Glibenclamide	0.75	–	2.5	<0.01[a]	<0.0017	<0.0048	1.0	–
	Repaglinide	2.2	5.6	0.5	0.02	0.0003	0.00099	1.0	1.0
	Rosiglitazone	6.0	11	8	0.002[a]	0.017	0.031	1.0	1.0
Ca^{2+} channel blockers	Diltiazem	>100	190	60	0.32	0.046	2.9	1.0	1.0
	Mibefradil	95	180	100	0.01	0.019	0.16	1.0	1.0
	Nisoldipine	7.4	>100	10	0.08	0.00098	0.14	1.0	1.0
Azoles	Fluconazole	>100	>100	100	0.89	7.7	28	<1.3	<1.3
	Itraconazole	>100	>30	100	0.002[a]	0.0008	0.20	1.0	1.0
	Ketoconazole	19	19	200	0.01	0.066	0.30	1.0	1.0

(continued)

Table 6.1 (continued)

Pharmacological action	Name	K_i or IC_{50} value for OATP1B1 (μM)	K_i or IC_{50} value for OATP1B3 (μM)	Dose (mg)	f_B	$I_{u,max}$ (μM)	$I_{u,in,max}$ (μM)	R value for OATP1B1	R value for OATP1B3
Antibiotics	Rifampicin	1.3	1.2	600	0.11	0.87	6.4	**5.9**	**6.3**
	Trimethoprim	>100	>100	160	0.42	4.2	20	<1.2	<1.2
Uricosuric drug	Probenecid	76	130	1,000	0.11	12	35	1.5	1.3
	Sulfinpyrazone	32	47	200	0.02	0.96	1.6	1.1	1.0
Thrombopoietin receptor agonist	Eltrombopag	2.7	ND	75	<0.01[a]	<0.18	<0.30	1.1	–
Choleretic drug	Ursodeoxycholic acid	10	80	400	<0.3	<6.8	<28	**<3.8**	<1.4
Angiotensin II receptor antagonists	Telmisartan	0.44	0.81[c]	40	<0.01[a]	0.0015	0.050	1.1	1.1
	Valsartan	9.0	18[c]	40	0.06	0.19	0.53	1.1	1.0
Anti-hepatitis C virus drugs	Boceprevir	18	4.9	800	0.25	0.79	8.9	1.5	**2.8**
	Telaprevir	2.2	6.8	750	0.37	1.0	9.8	**5.5**	**2.4**

These parameters are cited from Yoshida et al. 2012, "Transportal" Web Database and package insert of each drug
[a]If f_B is less than 0.01, according to the reguratory guidances, f_B is regarded as 0.01 for the calculation of R values
[b]Gemfibrozil glucuronide; a major metabolite of gemfibrozil
[c]Reported K_m value

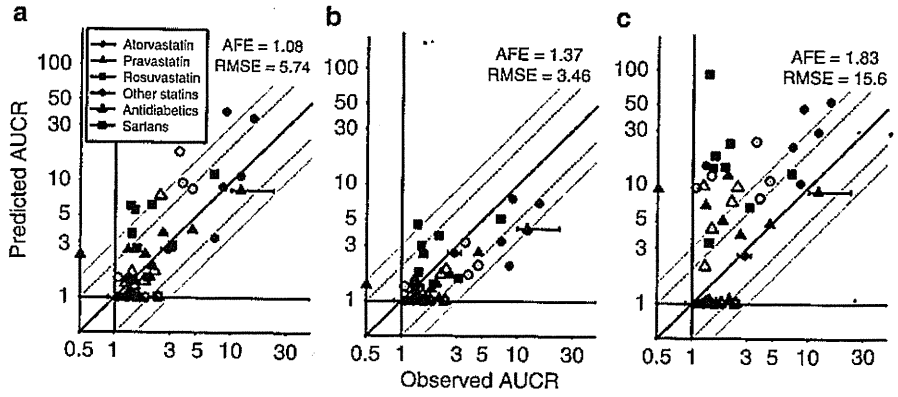

Fig. 6.5 Impact of the selection of inhibitor concentration used in a static model on the predictability of TP-DDIs involving OATP transporters (cited from Yoshida et al. 2012). Predictability of DDIs was compared when $I_{u,in,max}$ (**a**), $I_{u,max}$ (**b**), or I_{max} (**c**) was used in a static model. Each *point* and *horizontal bar* represents the median, maximum, and minimum values of the observed AUC ratios for the same combination of drugs. The *solid*, *dashed*, and *dotted lines* represent the line of unity, the 50–200 % range, and the 33–300 % range of the observed AUC ratios, respectively. *AFE* average fold error, *RMSE* root mean squared error

CYP-mediated DDIs (Ito et al. 2002), the use of $I_{u,in,max}$ minimized the number of false-negative predictions. Moreover, when I_{max} was used, the number of false-positive predictions increased because several clinically relevant OATP inhibitors showed a very low protein-unbound fraction and the discrepancy between the total and unbound concentrations of such inhibitors was large.

In the third assumption, the maximum inhibitory effects of biliary efflux transporters and/or metabolic enzymes as well as uptake transporters on the decreased hepatic intrinsic clearance were considered. As mentioned above, if the hepatic uptake clearance alone determines the overall intrinsic hepatic clearance, the ratio of the overall intrinsic clearance in the presence of inhibitor to that in its absence can be described by (6.14). On the other hand, when the β value is much smaller than 1, the ratio is described by (6.15) or (6.16) if compounds are eliminated from the body by extensive metabolism or biliary excretion in an unchanged form, respectively. Thus, to consider the maximum inhibitory effects on multiple processes when substrate drugs are recognized by uptake transporters, efflux transporters, and/or metabolic enzymes, the product of the R values for uptake and excretion and/or metabolism using the $I_{u,in,max}$ value should be considered (6.31) (Ueda et al. 2001).

$$\frac{CL_{int,all}(+\text{inhibitor})}{CL_{int,all}(-\text{inhibitor})} \sim \frac{1}{R_{inf}} \frac{1}{R_{ex/met}} < \frac{1}{1+\frac{I_{u,in,max}}{K_{i,inf}}} \frac{1}{1+\frac{I_{u,in,max}}{K_{i,ex/met}}} \quad (6.31)$$

The number of false-negative predictions can be minimized when the product of R values is used for the DDI prediction rather than just the R value for uptake (16 → 11 studies). In particular, DDI cases between fluconazole and CYP2C9 substrates (glimepiride, nateglinide, irbesartan) are predicted correctly when we consider the maximum inhibitory effects of both uptake and metabolism. This is reasonable because the clinical dose of fluconazole does not cause the inhibition of OATP-mediated uptake, but may inhibit CYP2C9-mediated metabolism. This may imply that the β values of these substrates are not close to 1, although this needs to be confirmed. However, the prediction accuracy was the highest when only the R value for uptake was used (76 and 90 % for predictions within two- to threefold of the observed the AUCR values, respectively). We note that the concentrated uptake of inhibitor drugs is not assumed in this equation because it is possible that the intracellular unbound concentration may be higher than the unbound concentration in the blood. If the $K_{p,uu}$ value in the liver is estimated from in vitro experiments, $I_{u,in,max} \times K_{p,uu}$ should be used instead of $I_{u,in,max}$ for the calculation of the maximum $R_{ex/met}$ value.

In the current FDA draft guidance on DDIs (US Food and Drug Administration (FDA) 2012), when the drug candidates are inhibitors of hepatic OATPs, in the first step, if the I_{max}/K_i value is more than 0.1, the R value should be calculated using the $I_{u,in,max}$ value. If the R value is more than 1.25, in vivo clinical DDI studies with OATP substrate drugs (e.g., rosuvastatin) are recommended. On the other hand, in the EMA guideline on DDIs (European Medicines Agency (EMA) 2010), the threshold for the R value calculated using the $I_{u,in,max}$ value is 1.04, which is stricter than that contained in the FDA draft guidance. The performance of the current DDI prediction method may need to be evaluated and optimized in future.

6.4.3 *Prediction of TP-DDIs in the Liver with a Dynamic Model*

Differing from a static model, a dynamic model enables one to predict the extent of the change in the AUC accurately because it considers the time-dependent change in the inhibition potency of inhibitors on the intrinsic hepatic clearance of substrates. The parameter settings are key to constructing a good model for describing the pharmacokinetic character of drugs appropriately (Shitara et al. 2013; Yoshida et al. 2013; Barton et al. 2013; Zamek-Gliszczynski et al. 2013; Rowland et al. 2011). Even a simple compartment model, which partly omits the physiological structure and machinery of detoxification of xenobiotics, can roughly reproduce the time profile of the plasma concentration of a drug. However, this is no longer useful if one wishes to consider the influence of the functional change of a single molecule on the pharmacokinetics of drugs because of the lack of parameters. Conversely, recent findings on the molecular mechanisms of pharmacokinetics allow one to create a very complex mechanistic model with many model parameters. However, it is difficult to set all the model parameters rationally, and there is a kind of trade-off for issues that have no clear answer.

The methods for setting the parameters are classified into two approaches. One approach is to determine the parameters using a simple scale-up method from only the in vitro experimental results; this is named the "bottom-up approach." For example, based on the traditional strategy of in vitro–in vivo extrapolation, in vivo metabolic intrinsic clearance can be predicted from in vitro metabolic clearance in liver microsomes by multiplying the in vitro clearance by the liver weight per unit body weight (e.g., 24.3 g liver/kg in humans) and the microsomal protein amount per unit liver weight (e.g., 40 mg protein/g liver in humans). However, some researchers have noted that a simple scale-up method cannot be effective for accurately predicting the in vivo parameters. For example, Houston et al. collected in vitro intrinsic clearances of 89 compounds estimated with human cryopreserved hepatocytes and carefully scaled up the in vitro data to predict the vivo hepatic intrinsic clearance based on physiologically based scaling factors (Houston et al. 2012). They observed systematic underprediction of the intrinsic hepatic clearance. Naritomi et al. showed that introduction of drug-specific empirical scaling factors, which are defined as the ratio of intrinsic clearance in vivo to that predicted from in vitro experiments in rats, can be useful for improving the prediction of hepatic intrinsic clearance of different species (Naritomi et al. 2001).

For the uptake transporters, Menochet et al. compared the predicted intrinsic hepatic clearances of six OATP substrates from in vitro uptake assays with cultured human hepatocytes and the observed clearance (Menochet et al. 2012). The predicted clearances of these compounds was 17-fold smaller than that observed on average, indicating that compound- and donor-specific empirical scaling factors are needed to predict the in vivo hepatic intrinsic clearances better. One strategy to determining an empirical scaling factor for each process is to estimate the ratio of in vivo intrinsic clearance to the in vitro predicted clearance in animal experiments and then to apply the same ratio to the prediction of human pharmacokinetics. Watanabe et al. succeeded in the prediction of the pharmacokinetics of pravastatin in rats using a PBPK model, in which the liver was divided into five subcompartments to mimic the dispersion model and in its prediction in humans by using the same scaling factors for influx (3.7) and biliary excretion (21) clearances (Watanabe et al. 2009b). Poirier et al. constructed a PBPK model of valsartan in humans, which included the relative contribution of OATP1B1 and OATP1B3 to the overall hepatic uptake of valsartan. A good prediction of the human pharmacokinetics of valsartan was achieved when they used an empirical scaling factor for hepatic uptake of 5, which was optimized to match the plasma concentration and biliary excretion profile of valsartan in rats (Poirier et al. 2009). Several possible reasons for the differences between in vitro and in vivo systems can be considered such as the difference in the expression/function of several transporters/enzymes between cell systems and intact tissues. However, no one has presented a definitive hypothesis about the cause of the apparent discrepancy between in vitro and in vivo systems.

Another approach is to determine the parameters by fitting in vivo clinical data to an appropriate pharmacokinetic model, which is named the "top-down approach." Johns et al. tried to confirm the predictability of the human pharmacokinetics of seven OATP substrates from the in vitro parameters obtained with

sandwich-cultured human hepatocytes and a PBPK model. The simple use of in vitro parameters for the PBPK model led to an overprediction of the exposure for all compounds (Jones et al. 2012). The authors concluded that the drug-dependent scaling factors for each process that best explained the time profile of plasma concentration after the intravenous administration in humans were 12–161 for uptake clearance and 0.024–0.12 for biliary excretion clearance. Because this approach requires human clinical data, the model parameters cannot be set for drug candidates whose clinical data are not available. Thus, at the moment, because a universal method to determine the empirical scaling factors for each parameter is not available, a combination of "bottom-up" and "top-down" approaches should be applied to predict the pharmacokinetics of drugs.

Several studies have used PBPK modeling to predict complex DDI cases quantitatively. Kudo et al. tried to use PBPK modeling to explain the complex DDI of repaglinide with gemfibrozil and itraconazole (Kudo et al. 2013). In this clinical case, the plasma AUC of repaglinide was increased by 1.4- and 8.1-fold by the coadministration of itraconazole and gemfibrozil, respectively (Niemi et al. 2003). By contrast, the plasma AUC of repaglinide increased by 19.4-fold when coadministered with both itraconazole and gemfibrozil (Niemi et al. 2003). Because repaglinide is a substrate of CYP2C8, CYP3A4, and OATP1B1, the cause of this DDI relates to the potent inhibition of CYP3A4 by itraconazole, the mechanism-based inhibition of CYP2C8 by gemfibrozil glucuronide, and the inhibition of OATP1B1 by gemfibrozil and its glucuronide. The cause of such observations is sometimes recognized as a "synergistic" inhibitory effect by the combined use of itraconazole and gemfibrozil. Kudo et al. constructed simple PBPK models for itraconazole, gemfibrozil and its glucuronide, and repaglinide (as shown Fig. 6.6a), and they optimized multiple model parameters by fitting the time profiles of the plasma concentrations of these drugs to the PBPK models (Fig. 6.6b) (Kudo et al. 2013). The optimized K_i values of itraconazole for CYP3A4, gemfibrozil and its glucuronide for OATP1B1, and the fraction of repaglinide metabolized by CYP2C8 were similar to the in vitro experimental results. Thus, the PBPK model analyses showed that this complex TP-DDI case can be explained simply by the multiple inhibitions of the clearance pathways of repaglinide without having to consider any empirical "synergistic" effect.

Varma et al. also used PBPK modeling of repaglinide to explain the multiple clinical DDI cases based on the available in vitro information. They initially tried to use the in vitro kinetic parameters of metabolism and transport of repaglinide obtained from experiments with hepatic microsomes and sandwich-cultured hepatocytes as model parameters. However, the use of in vitro intrinsic clearance for sinusoidal active uptake resulted in the overestimation of the systemic exposure of repaglinide, and a scaling factor of 16.9 was finally applied to explain the pharmacokinetics of repaglinide. Using this PBPK model, they succeeded in accurately predicting the AUC ratio of repaglinide after coadministration of ketoconazole, itraconazole, cyclosporine A, or gemfibrozil in previous clinical reports. They successfully predicted the dosing–time-dependent pharmacokinetic interaction of repaglinide with rifampicin by using a similar PBPK model incorporating the induction of CYP3A4 and reversible inhibition of OATP1B1 (Varma et al. 2013). Varma

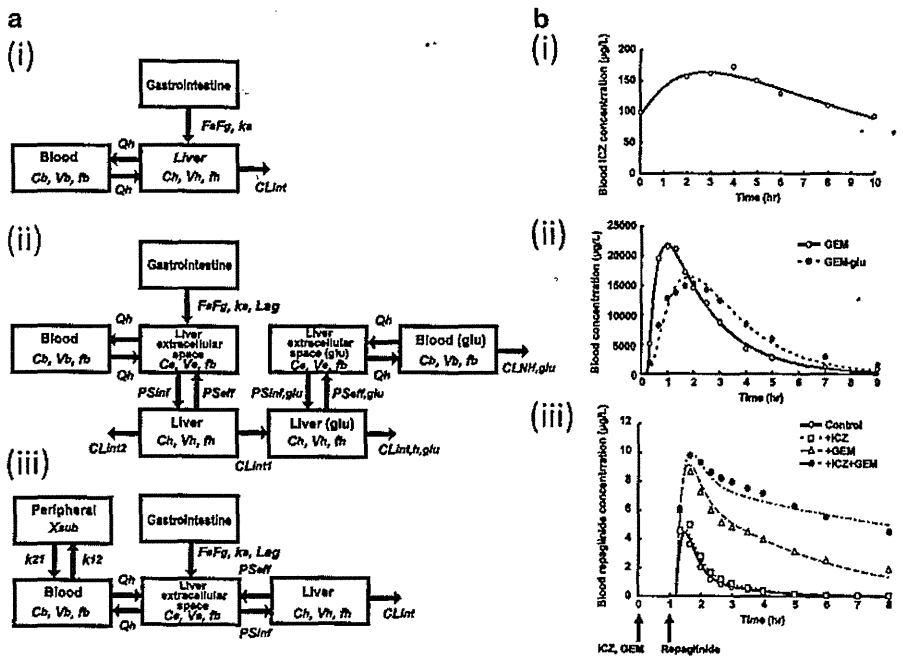

Fig. 6.6 Prediction of DDI of repaglinide with itraconazole and gemfibrozil by a dynamic PBPK model (cited from Kudo et al. 2013). (**a**) Structure of simple PBPK models for (*i*) itraconazole, (*ii*) gemfibrozil and its glucuronide, and (*iii*) repaglinide. (**b**) Predicted and observed time profiles of the blood concentration of (*i*) itraconazole, (*ii*) gemfibrozil and its glucuronide, and (*iii*) repaglinide with the coadministration of itraconazole (*open squares*), gemfibrozil (*open triangles*), and combination use of itraconazole and gemfibrozil (*closed circles*) or without any coadministered drugs (*open circles*). The overlaid lines in each figure represent the predicted time profiles of blood concentration of drugs based on PBPK model

et al. also used a PBPK model to perform a similar type of DDI prediction for pravastatin (Varma et al. 2012). The time profiles of pravastatin were reproduced by the PBPK model with scaling factors of sinusoidal active uptake and canalicular efflux of 31 and 0.17, respectively, which related the model parameters to in vitro parameters in sandwich-cultured hepatocytes. Interestingly, they were successful at predicting the TP-DDIs with gemfibrozil and rifampicin, but the DDI with cyclosporine A was underpredicted by the PBPK model, suggesting that the in vivo K_i value might be smaller than the in vitro K_i value obtained from the in vitro inhibition assay (Varma et al. 2012). This may reflect the decreased K_i value by preincubation with cyclosporine A.

Gertz et al. also tried to predict the TP-DDI of repaglinide with cyclosporine A using a PBPK model. The prediction was successful when considering the preincubation effect of cyclosporine A on the K_i value and almost complete inhibition of P-gp and CYP3A4 in the intestine, whereas the effects of OATP1B1 inhibition by AM1, a major metabolite of cyclosporine A, played a minor role in the accurate DDI prediction (Gertz et al. 2013).

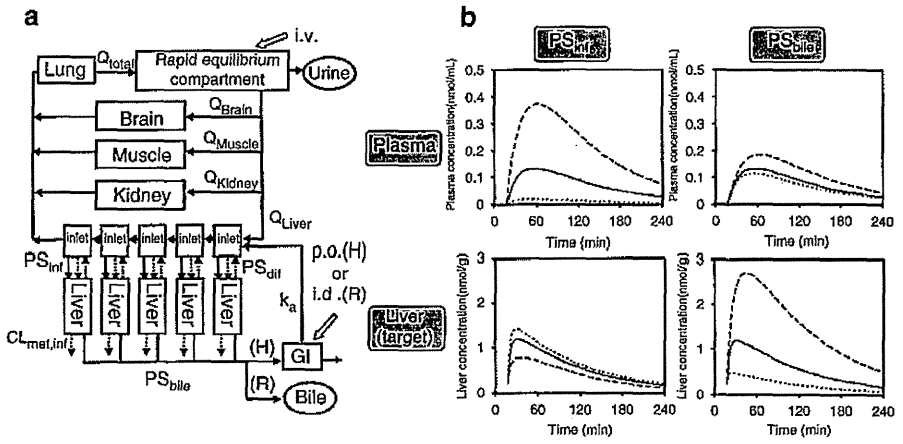

Fig. 6.7 Impact of the change in the hepatic influx and biliary excretion on the plasma and hepatic concentration of pravastatin based on the results of PBPK modeling (cited from Watanabe et al. 2009b). (**a**) Schematic diagram of the PBPK model predicting the concentration-time profiles of pravastatin. The liver compartment was divided into five compartments to mimic the dispersion model. (*H*) humans, (*R*) Rats, The enterohepatic circulation was incorporated in the case of humans. (**b**) Effects of changes in the transporter activity of hepatic influx and biliary efflux on the time profiles of plasma and liver (target organ) concentrations of pravastatin in humans. Plasma and liver concentrations after oral administration (40 mg) were simulated using the PBPK model with varying hepatic transport activities over a 1/3- to 3-fold range of the optimized values (*solid line*, initial; *dashed line*, ×1/3; *dotted line*, ×3)

One of the great advantages of the dynamic model approach is that one may simulate the time profiles of plasma and tissue concentrations of the substrates and inhibitor drugs when some model parameters are changed artificially once an appropriate PBPK model is obtained. This helps decrease the need for clinical studies. We can also perform a sensitivity analysis to search for the important parameters that markedly modify the plasma and tissue concentrations of drugs in the PBPK model. Watanabe et al. showed the impact of influx clearance and biliary efflux clearance on the plasma and hepatic concentrations of pravastatin by sensitivity analysis (Fig. 6.7) (Watanabe et al. 2009b). As observed for statins, the plasma concentration determines muscle toxicity, whereas the hepatic concentration is related to the pharmacological effect. In their analyses, decreasing the influx clearance markedly increased the plasma concentration of pravastatin, whereas its hepatic concentration did not change much. These simulation results are similar to the clinical observations that the pharmacological effects of statins are not affected much in subjects with the *SLCO1B1* 521T>C allele (Martin et al. 2012), which was reported to decrease the transport function, whereas the risk of muscle toxicity increases significantly in those with this allele (Link et al. 2008). By contrast, decreasing the biliary efflux transport did not change the plasma concentration, but markedly increased the hepatic concentration, suggesting the increased pharmacological effects of pravastatin. These kinds of findings can be realized only by using the PBPK-modeling approach.

6.5 Conclusions

This chapter has discussed novel methods for hepatic TP-DDI prediction and their applications. Selection of the prediction methods depends on the situation. In the early stage of drug development, because information about the pharmacokinetic properties of drugs is not readily available, a static model using the $I_{u,in,max}$ value is useful for sensitively identifying DDI risk of new chemical entities. After obtaining the pharmacokinetics of a new chemical entity in humans, the kinetic parameters for the PBPK model are optimized by using both in vitro experimental results ("bottom–up" approach) and clinical pharmacokinetic information ("top–down" approach). At present, although a complete bottom–up approach is ideal because the prediction of pharmacokinetics is realized only by using in vitro data without any clinical data, it is difficult to say whether the model parameters can be estimated by a simple scale-up of in vitro results. Several reports have shown the need for compound-dependent nonphysiological empirical scaling factors for each intrinsic clearance of drugs (Barton et al. 2013; Houston et al. 2012; Zamek-Gliszczynski et al. 2013). The mechanisms underlying discrepancies between in vivo and in vitro systems are not understood fully. In the validation of the PBPK model, only the plasma and urine concentrations, but not the tissue concentrations, of drugs are available in humans. Thus, the validity of multiple model parameters cannot be guaranteed by the limited information of drug concentration, and many sets of parameters might explain the time profiles of drug concentrations in plasma and urine. To overcome this problem, noninvasive imaging techniques such as positron emission tomography (PET) are powerful approaches to measure directly the tissue concentration of drugs. Takashima et al. characterized the transporter-mediated hepatobiliary transport of [^{11}C]-15*R*-TIC and found that the coadministration of rifampicin decreased the intrinsic clearance of both the hepatic uptake and biliary efflux of radioactivity (Takashima et al. 2012). Our group has proposed several kinds of PET ligands, which are substrates of selective transporters and can be used to characterize their hepatic transport properties in humans. This kind of information will provide clues to identify a set of optimized model parameters. In future, development of a pharmacodynamic model that incorporates the dynamics of the molecular machinery of the pharmacodynamic/toxicological actions of drugs based on the experimental approach combined with the dynamic PBPK model will provide the opportunity to predict quantitatively the real-time pharmacological actions of drugs under specific conditions.

References

Allen JD, van Loevezijn A, Lakhai JM, van der Valk M, van Tellingen O, Reid G, Schellens JH, Koomen GJ, Schinkel AH (2002) Potent and specific inhibition of the breast cancer resistance protein multidrug transporter in vitro and in mouse intestine by a novel analogue of fumitremorgin C. Mol Cancer Ther 1(6):417–425

Amundsen R, Christensen H, Zabihyan B, Asberg A (2010) Cyclosporine A, but not tacrolimus, shows relevant inhibition of organic anion-transporting protein 1B1-mediated transport of atorvastatin. Drug Metab Dispos 38(9):1499–1504. doi:10.1124/dmd.110.032268

Barton HA, Lai Y, Goosen TC, Jones HM, El-Kattan AF, Gosset JR, Lin J, Varma MV (2013) Model-based approaches to predict drug–drug interactions associated with hepatic uptake transporters: preclinical, clinical and beyond. Expert Opin Drug Metab Toxicol 9(4):459–472. doi:10.1517/17425255.2013.759210

Campbell SD, de Morais SM, Xu JJ (2004) Inhibition of human organic anion transporting polypeptide OATP 1B1 as a mechanism of drug-induced hyperbilirubinemia. Chem Biol Interact 150(2):179–187. doi:10.1016/j.cbi.2004.08.008

Crespi CL, Penman BW (1997) Use of cDNA-expressed human cytochrome P450 enzymes to study potential drug–drug interactions. Adv Pharmacol 43:171–188

Cui Y, Konig J, Leier I, Buchholz U, Keppler D (2001) Hepatic uptake of bilirubin and its conjugates by the human organic anion transporter SLC21A6. J Biol Chem 276(13):9626–9630. doi:10.1074/jbc.M004968200

Dantzig AH, Shepard RL, Cao J, Law KL, Ehlhardt WJ, Baughman TM, Bumol TF, Starling JJ (1996) Reversal of P-glycoprotein-mediated multidrug resistance by a potent cyclopropyldibenzosuberane modulator, LY335979. Cancer Res 56(18):4171–4179

European Medicines Agency (EMA) (2010) Guideline on the investigation of drug interactions. http://www.ema.europa.eu/docs/en_GB/document_library/Scientific_guideline/2010/05/WC500090112.pdf

Gertz M, Cartwright CM, Hobbs MJ, Kenworthy KE, Rowland M, Houston JB, Galetin A (2013) Cyclosporine inhibition of hepatic and intestinal CYP3A4, uptake and efflux transporters: application of PBPK modeling in the assessment of drug–drug interaction potential. Pharm Res 30(3):761–780. doi:10.1007/s11095-012-0918-y

Hagenbuch B, Scharschmidt BF, Meier PJ (1996) Effect of antisense oligonucleotides on the expression of hepatocellular bile acid and organic anion uptake systems in Xenopus laevis oocytes. Biochem J 316(pt 3):901–904

Hirano M, Maeda K, Shitara Y, Sugiyama Y (2004) Contribution of OATP2 (OATP1B1) and OATP8 (OATP1B3) to the hepatic uptake of pitavastatin in humans. J Pharmacol Exp Ther 311(1):139–146. doi:10.1124/jpet.104.068056

Hirano M, Maeda K, Shitara Y, Sugiyama Y (2006) Drug–drug interaction between pitavastatin and various drugs via OATP1B1. Drug Metab Dispos 34(7):1229–1236. doi:10.1124/dmd.106.009290

Houston JB, Rowland-Yeo K, Zanelli U (2012) Evaluation of the novel in vitro systems for hepatic drug clearance and assessment of their predictive utility. Toxicol In Vitro 26(8):1265–1271. doi:10.1016/j.tiv.2011.12.016

Ishigami M, Tokui T, Komai T, Tsukahara K, Yamazaki M, Sugiyama Y (1995) Evaluation of the uptake of pravastatin by perfused rat liver and primary cultured rat hepatocytes. Pharm Res 12(11):1741–1745

Ishiguro N, Maeda K, Kishimoto W, Saito A, Harada A, Ebner T, Roth W, Igarashi T, Sugiyama Y (2006) Predominant contribution of OATP1B3 to the hepatic uptake of telmisartan, an angiotensin II receptor antagonist, in humans. Drug Metab Dispos 34(7):1109–1115. doi:10.1124/dmd.105.009175

Ito K, Iwatsubo T, Kanamitsu S, Ueda K, Suzuki H, Sugiyama Y (1998) Prediction of pharmacokinetic alterations caused by drug–drug interactions: metabolic interaction in the liver. Pharmacol Rev 50(3):387–412

Ito K, Chiba K, Horikawa M, Ishigami M, Mizuno N, Aoki J, Gotoh Y, Iwatsubo T, Kanamitsu S, Kato M, Kawahara I, Niinuma K, Nishino A, Sato N, Tsukamoto Y, Ueda K, Itoh T, Sugiyama Y (2002) Which concentration of the inhibitor should be used to predict in vivo drug interactions from in vitro data? AAPS PharmSci 4(4):E25. doi:10.1208/ps040425

Jigorel E, Le Vee M, Boursier-Neyret C, Bertrand M, Fardel O (2005) Functional expression of sinusoidal drug transporters in primary human and rat hepatocytes. Drug Metab Dispos 33(10):1418–1422. doi:10.1124/dmd.105.004762

Jones HM, Barton HA, Lai Y, Bi YA, Kimoto E, Kempshall S, Tate SC, El-Kattan A, Houston JB, Galetin A, Fenner KS (2012) Mechanistic pharmacokinetic modeling for the prediction of transporter-mediated disposition in humans from sandwich culture human hepatocyte data. Drug Metab Dispos 40(5):1007–1017. doi:10.1124/dmd.111.042994

Kindla J, Muller F, Mieth M, Fromm MF, Konig J (2011) Influence of non-steroidal anti-inflammatory drugs on organic anion transporting polypeptide (OATP) 1B1- and OATP1B3-mediated drug transport. Drug Metab Dispos 39(6):1047–1053. doi:10.1124/dmd.110.037622

Kotani N, Maeda K, Watanabe T, Hiramatsu M, Gong LK, Bi YA, Takezawa T, Kusuhara H, Sugiyama Y (2011) Culture period-dependent changes in the uptake of transporter substrates in sandwich-cultured rat and human hepatocytes. Drug Metab Dispos 39(9):1503–1510. doi:10.1124/dmd.111.038968

Kouzuki H, Suzuki H, Ito K, Ohashi R, Sugiyama Y (1998) Contribution of sodium taurocholate co-transporting polypeptide to the uptake of its possible substrates into rat hepatocytes. J Pharmacol Exp Ther 286(2):1043–1050

Kouzuki H, Suzuki H, Ito K, Ohashi R, Sugiyama Y (1999) Contribution of organic anion transporting polypeptide to uptake of its possible substrates into rat hepatocytes. J Pharmacol Exp Ther 288(2):627–634

Kudo T, Hisaka A, Sugiyama Y, Ito K (2013) Analysis of the repaglinide concentration increase produced by gemfibrozil and itraconazole based on the inhibition of the hepatic uptake transporter and metabolic enzymes. Drug Metab Dispos 41(2):362–371. doi:10.1124/dmd.112.049460

Kusunoki N, Takara K, Tanigawara Y, Yamauchi A, Ueda K, Komada F, Ku Y, Kuroda Y, Saitoh Y, Okumura K (1998) Inhibitory effects of a cyclosporin derivative, SDZ PSC 833, on transport of doxorubicin and vinblastine via human P-glycoprotein. Jpn J Cancer Res 89(11):1220–1228

Li N, Bi YA, Duignan DB, Lai Y (2009) Quantitative expression profile of hepatobiliary transporters in sandwich cultured rat and human hepatocytes. Mol Pharm 6(4):1180–1189. doi:10.1021/mp900044x

Liao M, Raczynski AR, Chen M, Chuang BC, Zhu Q, Shipman R, Morrison J, Lee D, Lee FW, Balani SK, Xia CQ (2010) Inhibition of hepatic organic anion-transporting polypeptide by RNA interference in sandwich-cultured human hepatocytes: an in vitro model to assess transporter-mediated drug–drug interactions. Drug Metab Dispos 38(9):1612–1622. doi:10.1124/dmd.110.032995

Group SC, Link E, Parish S, Armitage J, Bowman L, Heath S, Matsuda F, Gut I, Lathrop M, Collins R (2008) SLCO1B1 variants and statin-induced myopathy—a genomewide study. N Engl J Med 359(8):789–799. doi:10.1056/NEJMoa0801936

Maeda K, Ikeda Y, Fujita T, Yoshida K, Azuma Y, Haruyama Y, Yamane N, Kumagai Y, Sugiyama Y (2011) Identification of the rate-determining process in the hepatic clearance of atorvastatin in a clinical cassette microdosing study. Clin Pharmacol Ther 90(4):575–581. doi:10.1038/clpt.2011.142

Martin NG, Li KW, Murray H, Putt W, Packard CJ, Humphries SE (2012) The effects of a single nucleotide polymorphism in SLCO1B1 on the pharmacodynamics of pravastatin. Br J Clin Pharmacol 73(2):303–306. doi:10.1111/j.1365-2125.2011.04090.x

Matsushima S, Maeda K, Ishiguro N, Igarashi T, Sugiyama Y (2008) Investigation of the inhibitory effects of various drugs on the hepatic uptake of fexofenadine in humans. Drug Metab Dispos 36(4):663–669. doi:10.1124/dmd.107.017814

Menochet K, Kenworthy KE, Houston JB, Galetin A (2012) Use of mechanistic modeling to assess interindividual variability and interspecies differences in active uptake in human and rat hepatocytes. Drug Metab Dispos 40(9):1744–1756. doi:10.1124/dmd.112.046193

Nakai D, Nakagomi R, Furuta Y, Tokui T, Abe T, Ikeda T, Nishimura K (2001) Human liver-specific organic anion transporter, LST-1, mediates uptake of pravastatin by human hepatocytes. J Pharmacol Exp Ther 297(3):861–867

Naritomi Y, Terashita S, Kimura S, Suzuki A, Kagayama A, Sugiyama Y (2001) Prediction of human hepatic clearance from in vivo animal experiments and in vitro metabolic studies with liver microsomes from animals and humans. Drug Metab Dispos 29(10):1316–1324

Niemi M, Backman JT, Neuvonen M, Neuvonen PJ (2003) Effects of gemfibrozil, itraconazole, and their combination on the pharmacokinetics and pharmacodynamics of repaglinide: potentially hazardous interaction between gemfibrozil and repaglinide. Diabetologia 46(3):347–351. doi:10.1007/s00125-003-1034-7

Noe J, Portmann R, Brun ME, Funk C (2007) Substrate-dependent drug–drug interactions between gemfibrozil, fluvastatin and other organic anion-transporting peptide (OATP) substrates on OATP1B1, OATP2B1, and OATP1B3. Drug Metab Dispos 35(8):1308–1314. doi:10.1124/dmd.106.012930

Ohtsuki S, Uchida Y, Kubo Y, Terasaki T (2011) Quantitative targeted absolute proteomics-based ADME research as a new path to drug discovery and development: methodology, advantages, strategy, and prospects. J Pharm Sci 100(9):3547–3559. doi:10.1002/jps.22612

Oostendorp RL, van de Steeg E, van der Kruijssen CM, Beijnen JH, Kenworthy KE, Schinkel AH, Schellens JH (2009) Organic anion-transporting polypeptide 1B1 mediates transport of Gimatecan and BNP1350 and can be inhibited by several classic ATP-binding cassette (ABC) B1 and/or ABCG2 inhibitors. Drug Metab Dispos 37(4):917–923. doi:10.1124/dmd.108.024901

Poirier A, Cascais AC, Funk C, Lave T (2009) Prediction of pharmacokinetic profile of valsartan in human based on in vitro uptake transport data. J Pharmacokinet Pharmacodyn 36(6):585–611. doi:10.1007/s10928-009-9139-3

Rippin SJ, Hagenbuch B, Meier PJ, Stieger B (2001) Cholestatic expression pattern of sinusoidal and canalicular organic anion transport systems in primary cultured rat hepatocytes. Hepatology 33(4):776–782. doi:10.1053/jhep.2001.23433

Rowland M, Peck C, Tucker G (2011) Physiologically-based pharmacokinetics in drug development and regulatory science. Annu Rev Pharmacol Toxicol 51:45–73. doi:10.1146/annurev-pharmtox-010510-100540

Shitara Y, Horie T, Sugiyama Y (2006) Transporters as a determinant of drug clearance and tissue distribution. Eur J Pharm Sci 27(5):425–446. doi:10.1016/j.ejps.2005.12.003

Shitara Y, Nagamatsu Y, Wada S, Sugiyama Y, Horie T (2009) Long-lasting inhibition of the transporter-mediated hepatic uptake of sulfobromophthalein by cyclosporin a in rats. Drug Metab Dispos 37(6):1172–1178. doi:10.1124/dmd.108.025544

Shitara Y, Maeda K, Ikejiri K, Yoshida K, Horie T, Sugiyama Y (2013) Clinical significance of organic anion transporting polypeptides (OATPs) in drug disposition: their roles in hepatic clearance and intestinal absorption. Biopharm Drug Dispos 34(1):45–78. doi:10.1002/bdd.1823

Soars MG, Grime K, Sproston JL, Webborn PJ, Riley RJ (2007) Use of hepatocytes to assess the contribution of hepatic uptake to clearance in vivo. Drug Metab Dispos 35(6):859–865. doi:10.1124/dmd.106.014464

Soars MG, Barton P, Ismair M, Jupp R, Riley RJ (2012) The development, characterization, and application of an OATP1B1 inhibition assay in drug discovery. Drug Metab Dispos 40(8):1641–1648. doi:10.1124/dmd.111.042382

Tachibana T, Kato M, Watanabe T, Mitsui T, Sugiyama Y (2009) Method for predicting the risk of drug–drug interactions involving inhibition of intestinal CYP3A4 and P-glycoprotein. Xenobiotica 39(6):430–443. doi:10.1080/00498250902846252

Takashima T, Kitamura S, Wada Y, Tanaka M, Shigihara Y, Ishii H, Ijuin R, Shiomi S, Nakae T, Watanabe Y, Cui Y, Doi H, Suzuki M, Maeda K, Kusuhara H, Sugiyama Y, Watanabe Y (2012) PET imaging-based evaluation of hepatobiliary transport in humans with (15R)-11C-TIC-Me. J Nucl Med 53(5):741–748. doi:10.2967/jnumed.111.098681

Tian X, Zamek-Gliszczynski MJ, Zhang P, Brouwer KL (2004) Modulation of multidrug resistance-associated protein 2 (Mrp2) and Mrp3 expression and function with small interfering RNA in sandwich-cultured rat hepatocytes. Mol Pharmacol 66(4):1004–1010. doi:10.1124/mol.66.4

Ueda K, Kato Y, Komatsu K, Sugiyama Y (2001) Inhibition of biliary excretion of methotrexate by probenecid in rats: quantitative prediction of interaction from in vitro data. J Pharmacol Exp Ther 297(3):1036–1043

Umehara K, Camenisch G (2012) Novel in vitro–in vivo extrapolation (IVIVE) method to predict hepatic organ clearance in rat. Pharm Res 29(2):603–617. doi:10.1007/s11095-011-0607-2

US Food and Drug Administration (FDA) (2012) Guidance for industry drug interaction studies–study design, data analysis, implications for dosing, and labeling recommendations. http://www.fda.gov/downloads/Drugs/GuidanceComplianceRegulatoryInformation/Guidances/UCM292362.pdf

Varma MV, Lai Y, Feng B, Litchfield J, Goosen TC, Bergman A (2012) Physiologically based modeling of pravastatin transporter-mediated hepatobiliary disposition and drug–drug interactions. Pharm Res 29(10):2860–2873. doi:10.1007/s11095-012-0792-7

Varma MV, Lin J, Bi YA, Rotter CJ, Fahmi OA, Lam J, El-Kattan AF, Goosen TC, Lai Y (2013) Quantitative prediction of repaglinide-rifampicin complex drug interactions using dynamic and static mechanistic models: delineating differential CYP3A4 induction and OATP1B1 inhibition potential of rifampicin. Drug Metab Dispos. doi:10.1124/dmd.112.050583

Watanabe T, Maeda K, Kondo T, Nakayama H, Horita S, Kusuhara H, Sugiyama Y (2009a) Prediction of the hepatic and renal clearance of transporter substrates in rats using in vitro uptake experiments. Drug Metab Dispos 37(7):1471–1479. doi:10.1124/dmd.108.026062

Watanabe T, Kusuhara H, Maeda K, Shitara Y, Sugiyama Y (2009b) Physiologically based pharmacokinetic modeling to predict transporter-mediated clearance and distribution of pravastatin in humans. J Pharmacol Exp Ther 328(2):652–662. doi:10.1124/jpet.108.146647

Watanabe T, Kusuhara H, Maeda K, Kanamaru H, Saito Y, Hu Z, Sugiyama Y (2010) Investigation of the rate-determining process in the hepatic elimination of HMG-CoA reductase inhibitors in rats and humans. Drug Metab Dispos 38(2):215–222. doi:10.1124/dmd.109.030254

Watanabe T, Kusuhara H, Watanabe T, Debori Y, Maeda K, Kondo T, Nakayama H, Horita S, Ogilvie BW, Parkinson A, Hu Z, Sugiyama Y (2011) Prediction of the overall renal tubular secretion and hepatic clearance of anionic drugs and a renal drug–drug interaction involving organic anion transporter 3 in humans by in vitro uptake experiments. Drug Metab Dispos 39(6):1031–1038. doi:10.1124/dmd.110.036129

Williamson B, Soars AC, Owen A, White P, Riley RJ, Soars MG (2013) Dissecting the relative contribution of OATP1B1-mediated uptake of xenobiotics into human hepatocytes using siRNA. Xenobiotica. doi:10.3109/00498254.2013.776194

Yabe Y, Galetin A, Houston JB (2011) Kinetic characterization of rat hepatic uptake of 16 actively transported drugs. Drug Metab Dispos 39(10):1808–1814. doi:10.1124/dmd.111.040477

Yoshida K, Maeda K, Sugiyama Y (2012) Transporter-mediated drug–drug interactions involving OATP substrates: predictions based on in vitro inhibition studies. Clin Pharmacol Ther 91(6):1053–1064. doi:10.1038/clpt.2011.351

Yoshida K, Maeda K, Sugiyama Y (2013) Hepatic and intestinal drug transporters: prediction of pharmacokinetic effects caused by drug–drug interactions and genetic polymorphisms. Annu Rev Pharmacol Toxicol 53:581–612. doi:10.1146/annurev-pharmtox-011112-140309

Yue W, Abe K, Brouwer KL (2009) Knocking down breast cancer resistance protein (Bcrp) by adenoviral vector-mediated RNA interference (RNAi) in sandwich-cultured rat hepatocytes: a novel tool to assess the contribution of Bcrp to drug biliary excretion. Mol Pharm 6(1):134–143. doi:10.1021/mp800100e

Zamek-Gliszczynski MJ, Lee CA, Poirier A, Bentz J, Chu X, Ellens H, Ishikawa T, Jamei M, Kalvass JC, Nagar S, Pang KS, Kowzekwa K, Swaan PW, Taub ME, Zhao P, Galetin A (2013) ITC recommendations on transporter kinetic parameter estimation and translational modeling of transport-mediated PK and DDIs in humans. Clin Pharmacol Ther. doi:10.1038/clpt.2013.45

Zelcer N, Huisman MT, Reid G, Wielinga P, Breedveld P, Kuil A, Knipscheer P, Schellens JH, Schinkel AH, Borst P (2003) Evidence for two interacting ligand binding sites in human multidrug resistance protein 2 (ATP binding cassette C2). J Biol Chem 278(26):23538–23544. doi:10.1074/jbc.M303504200

4 薬物相互作用ガイドラインの作成

❶ はじめに

現行指針である厚生労働省医薬局審査管理課長通知「薬物相互作用の検討方法について」[1]は，「薬物相互作用の発現を予測し，臨床試験実施の必要性を判断するための非臨床試験について基本的な考え方を示すとともに，ヒトにおける薬物相互作用発現の有無とその程度を確認するための臨床試験について具体的な方法や判断基準，並びに結果の解釈に関する留意事項を提示すること」を目的として，平成13年6月4日に通知された。11章より構成され，薬物の吸収，体内分布，シトクロムP450を主とする薬物代謝，排泄の各過程における薬物相互作用の概要と評価の原則が述べられており，さらに臨床試験が必要な場合について，実施のタイミングや試験デザインが記載されている。この指針については，当時の薬物相互作用ガイドライン検討班により詳細な解説がなされている[2]。

この指針は，策定当時としては最新の知見を取り入れた国際的にも先進的な指針であったが，すでに10年以上が経過し，現在の科学的知見から見ると足りないところも多く，効率的な医薬品開発や薬物相互作用を踏まえた適正使用を推進するうえで十分に活用されない可能性がでてきた。一方，米国食品医薬品庁（FDA）では薬物相互作用に関する新しいガイダンス案を平成18年に発表しており，さらにその改定案[3]を平成24年2月に発表した。また，欧州医薬品庁（EMA）でも平成24年6月に薬物相互作用に関する新ガイドライン[4]を発表し，平成25年1月から適用が開始された。これらは薬物動態を制御しているトランスポーターに関する試験，薬物動態モデル等による予測，定量的指標に基づく決定樹による臨床試験の必要性の判断や試験内容など最新の知見を反映したものとなっている。また，米国の新しいガイダンス案では，薬物動態学的に相互作用を生ずる機構に基づき関係する医薬品を分類し，グループごとに注意喚起する方法が取り入れられている。一方，より安全な薬物治療を患者に提供するためには，得られた相互作用情報の示し方も改定する必要がある。これらの状況に鑑み，本邦でも早急に新しいガイダンス策定のための検討を行う必要があると判断され，平成25年1月に厚生労働科学特別研究事業「医薬品開発における薬物相互作用の検討方法等に関する新ガイダンス作成のための研究（研究代表者・大野泰雄）」が発足し，改定のための検討が開始され，平成25年12月現在，改定案[5]のパブリックコメントが行われている。本稿においては，改定にあたっての基本的な考え方と改定案の骨子について記述した。

❷ 新ガイドライン案の内容について

2-1 新ガイドラインの目的と基本的考え方

新ガイドラインの目的は，「薬物相互作用の発現を予測し，臨床試験実施の必要性を判断するための非臨床試験，及びヒトにおける薬物相互作用の発現の有無とその程度を確認するための臨床試験について，具体的な方法や判断の基準，並びに試験結果の解釈や情報提供に関する一般的な指針を提示すること」とした。新ガイドラインの案では，従来と同様に吸収，分布，代謝，排泄，臨床試験という構成は堅持しているが，薬物トランスポーターの記載を，その評価方法の詳細を含め，大幅に増やすとともに，薬物代謝・トランスポーターの関わる相互作用の *in vitro* 評価と臨床試験の必要性について定量値を用いた決定樹を示し，判断の基準を明らかにした。また基質薬（被相互作用薬）としての評価と阻害薬・誘導薬（相互作用薬）との記載を分けて明確にした。さらに薬物代謝酵素の阻害や誘導では臨床試験の必要性について，静的薬物速度論（MSPK）モデルを利用したカットオフ基準による判断とともに，他のモデルによる評価を推奨する内容とした。また，臨床薬物相互作用試験の結果が薬物治療の現場で適切に活用されることを願い，薬物相互作用の強さによるクラス分けという考えを取り入れた試験結果の添付文書への反映に関する基本的な考え方も示した。さらに，国際的調和にも配慮した（表1）。

2-2 薬物代謝酵素が関わる薬物相互作用の予測

現行指針[1]では，薬物代謝酵素の阻害による血中濃度変動の予測は，「相互作用の過小評価（false negative）を避ける」観点から，肝臓入口における最大非結合形阻害薬濃度の推定値を用いて保守的に算出することを推奨している[6]。規制的側面から，薬物相互作用の予測に生理学的パラメータを組み込み定量的な判断基準を導入した点で，当時としては先進的な内容であり，

表1　EMAガイドライン，FDAガイダンス案，日本の指針と新ガイドライン案の比較表

項目	日本の現行指針（医薬審813号）	日本の新ガイドライン案	EMAガイドライン	FDAガイダンス案
適用範囲	医薬品，食品，生活習慣 薬物動態学的相互作用が主	医薬品（生物薬品を含む），飲食物，嗜好品（サプリメント等） 薬物動態学的相互作用が主	医薬品（生薬由来医薬品を含む），食品 薬物動態学的相互作用が主	医薬品（生物薬品を含む），食品，サプリメント 薬物動態学的相互作用が主
試験実施時期	原則，第Ⅲ相試験前	原則，第Ⅲ相試験前（*in vitro* 代謝試験は，第Ⅰ相試験前）	通常，第Ⅲ相試験前（*in vitro* 代謝試験は，第Ⅰ相試験前，トランスポーターは第Ⅲ相前）	記載なし
消化管吸収	pH変化，複合体形成，溶解性，消化管運動，薬物代謝関与（CYP3A4），トランスポーター関与（P-gp）	pH変化，複合体形成，溶解性，消化管運動，薬物代謝関与（CYP3A），トランスポーター関与（P-gp，BCRP）	pH変化，複合体形成，溶解性，消化管運動，薬物代謝関与（CYP3A），トランスポーター関与（P-gp等）	トランスポーター関与（P-gp，BCRP）
組織移行・体内分布	血漿蛋白結合，組織成分との結合，トランスポーターの関与	血漿蛋白結合，組織成分との結合，トランスポーターの関与	血漿蛋白結合（治療域狭く，非結合率1%未満等で重要），トランスポーターの関与	トランスポーターに関する一般的記載
主な検討対象薬物代謝酵素分子種	CYP1A2，2C9，2C19，2D6，3A4	CYP1A2，2B6，2C8，2C9，2C19，2D6，3A，UGT1A1，1A3，1A4，1A6，1A9，2B7，2B15	CYP1A2，2B6，2C8，2C9，2C19，2D6，3A，UGT1A1，2B7など	CYP1A2，2B6，2C8，2C9，2C19，2D6，3A，UGT1A1，1A3，1A4，1A6，1A9，2B7，2B15
解析対象とすべき酵素分子種の決定	記載なし	消失全体の25%以上に寄与する分子	消失全体の25%以上に寄与する分子	消失全体の25%以上に寄与する分子（複数酵素の合算の場合も）

項目	日本の現行指針（医薬審813号）	日本の新ガイドライン案	EMAガイドライン	FDAガイダンス案
解析対象とすべき代謝物の決定	未変化体の血中濃度が低く，多くが代謝物として存在する場合	被相互作用薬：*in vivo* における薬理活性が全体の50%以上を占める代謝物相互作用薬：AUCが未変化体の25%以上かつ薬物関連総曝露量の10%以上を占める代謝物	被相互作用薬：*in vivo* における薬理活性が全体の50%以上を占める代謝物相互作用薬：AUCが未変化体の25%以上かつ薬物関連総曝露量の10%以上を占める代謝物	被相互作用薬：AUCが未変化体の25%以上を占め，薬理/毒性学的作用を有する代謝物相互作用薬：AUCが未変化体の25%以上を占める分子
代謝関連の相互作用試験実施に関する決定樹の記載	記載なし	基質，阻害，誘導ごとに作成	基質，阻害，誘導ごとに作成	基質＋阻害＋誘導，UGT基質について作成
シトクロムP 450酵素の基質，阻害薬，誘導薬の例示（表）	*in vivo* の基質，指標薬，阻害薬，誘導薬 *in vitro* の指標薬，阻害薬	*in vivo* の薬物動態学的相互作用を受けやすい基質，阻害薬，誘導薬 *in vitro* のマーカー反応，阻害薬，誘導薬	*in vivo* の指標薬，阻害薬 *in vitro* のマーカー反応，阻害薬	*in vivo* の基質（感度が高い，治療域の狭い），阻害薬，誘導薬 *in vitro* の誘導薬
薬物動態モデル解析の内容	記載なし	カットオフ基準（basicモデル），メカニズムに基づく静的薬物速度論モデル（MSPKモデルと呼称），動的生理学的薬物速度論（PBPK）モデル	basicモデル，メカニズムに基づく静的薬物速度論モデル，動的生理学的薬物速度論（PBPK）モデル，誘導薬では，相対誘導スコア（RIS）法も	basicモデル，メカニズムに基づく静的薬物速度論モデル，動的生理学的薬物速度論（PBPK）モデル
代謝関連の相互作用薬として初期評価する際の薬物濃度基準	記載なし	総濃度のC_{max}（血中），投与量/250 mL（小腸）	非結合形濃度のC_{max}（血中），投与量/250 mL（小腸）	総濃度のC_{max}（血中），投与量/250 mL（小腸）

項目	日本の現行指針（医薬審813号）	日本の新ガイドライン案	EMAガイドライン	FDAガイダンス案
basic モデルにおける代謝阻害の相互作用判定基準	記載なし	R=1+[I]/Ki（[I]：前項の値，Ki：*in vitro* 阻害定数）		
		血中：1.1 小腸：11	血中：1.02 小腸：11	血中：1.1 小腸：11
生物薬品との相互作用	Q＆Aにケースバイケースでの対応と記載	複数の例を挙げて概念的に記載	他のガイドラインに記載（複数の例を挙げて，概念的に記載）	複数の例を挙げるとともに，決定樹を記載
主な検討対象トランスポーター分子種	P-gp	P-gp，BCRP，OATP1B1，OATP1B3，OAT1，OAT3，OCT2，MATE1，MATE2-K	P-gp，BCRP，OATP1B1，OATP1B3，OAT1，OAT3，OCT2（OCT1，MATE1，MATE2，BSEPも記載）	P-gp，BCRP，OATP1B1，OATP1B3，OAT1，OAT3，OCT2
トランスポーター関連の相互作用試験実施に関する決定樹の記載	記載なし	基質，阻害（各々P-gp/BCRP，肝トランスポーター，腎トランスポーター）	基質（腸管，消失（肝，腎）），阻害（具体名記載なし）	基質，阻害（各々P-gp/BCRP，肝トランスポーター，腎トランスポーター）
解析対象とすべきトランスポーター分子種の決定	特に記載なし	P-gp/BCRPの基質，肝又は腎排泄が総クリアランスの25％以上の場合，OATP1B1/OATP1B3またはOAT1/OAT3/OCT2/MATEs	P-gp/BCRPの基質で臨床的に重要な可能性有り．肝排泄が消失の25％以上の場合，OATP，腎または胆汁/消化管排泄が消失の25％以上の場合，関与する主要なトランスポーター分子	P-gp/BCRPの基質，肝または腎排泄が総クリアランスの25％以上の場合，OATP1B1/OATP1B3またはOAT1/OAT3/OCT2/MATEs

項目	日本の現行指針（医薬審813号）	日本の新ガイドライン案	EMAガイドライン	FDAガイダンス案
P-gp 阻害薬としての臨床試験の必要性判定基準	記載なし	総濃度 C_{max}/IC_{50} ≥0.1または（投与量/250 mL）/IC_{50}≥10	非結合体 C_{max}/K_i ≥ 0.02または（投与量/250 mL）/IC_{50}≥10	総濃度 C_{max}/IC_{50} ≥0.1または（投与量/250 mL）/IC_{50}≥10
トランスポーターの基質，阻害薬，誘導薬の例示（表）	記載なし	*in vivo* の基質，阻害薬，誘導薬，*in vivo* の典型基質，典型阻害薬，*in vitro* の典型基質，典型阻害薬	記載なし	*in vivo* の基質，阻害薬，誘導薬，CYP3A と P-gp の複合阻害薬
臨床試験における相互作用の判定基準	C_{max} および AUC の幾何平均比が80-125％の場合，相互作用なしと判断	C_{max} および AUC 等のの幾何平均比が80-125％の場合，相互作用なしと判断	記載なし	C_{max} および AUC の比が80-125％の場合，相互作用なしと判断
P450の阻害薬・誘導薬の強度分類	記載なし	強い，中程度，弱い	強い，中程度，弱い	強い，中程度，弱い
被相互作用薬の分類	記載なし	薬物動態学的相互作用を受けやすい，受けやすさが中程度，指標薬	指標薬	感度の高い，治療域の狭い
添付文書における薬物相互作用情報の提供方法	記載なし	概念的な基準に基づく記載方針，フォレストプロット等の図の活用	概念的な基準に基づく記載方針	概念的な基準に基づく記載方針，フォレストプロット等の図の活用

その後に公布された欧米規制当局の指針にもその考え方が受け継がれている。

本邦におけるガイドライン改定に当たっては，近年，さらに検証が進んだ薬物代謝酵素が関わる薬物相互作用の定量的予測手法を臨床試験の必要性判断に積極的に取り入れた。

1）ガイドライン改定の要点

薬物代謝酵素が関わる薬物相互作用に関して，現行指針から改定された主な項目と内容を以下に示す。

①時間依存的阻害（time-dependent inhibition；TDI）の評価方法

代謝酵素の失活を伴うため血中濃度上昇が顕著となる例が多いTDIの評価方法について記載するとともに，臨床における影響の予測結果は対象となる代謝酵素の分解速度定数（k_{deg}）に依存するため，文献値などを参考に感度分析を行うことを推奨した。

②酵素誘導の指標としてのmRNA発現量

上述したTDIを示す化合物では，酵素活性を指標とした場合に誘導能を過小評価することが懸念されることから，欧米規制当局の指針に合わせてmRNA発現量を指標とすることを推奨した。

③UDPグルクロン酸転移酵素（UGT）の分子種推定および阻害

UGTによる抱合代謝が主要代謝経路となる新薬の増加に加えて，UGT1A1の抱合活性低下をもたらす遺伝子多型が日本人に多いことから，相互作用を受ける側としての分子種推定と，相互作用を与える側としての阻害試験の必要性について記載した。

④遺伝子多型を考慮した臨床薬物相互作用試験の有用性

東アジア人で活性低下の頻度が高いCYP2C19やCYP2D6を例示し，遺伝子多型による影響やその民族差などを明らかにすることを念頭に，遺伝子型により層別化した臨床薬物相互作用試験の有用性に言及した。

⑤臨床薬物相互作用試験の必要性判断のための定量的基準

欧米規制当局の指針では，相互作用を受ける薬物のAUC上昇率の簡易予測式である「$R=1+[I]/Ki$，[I]とKiは各々阻害薬濃度と阻害定数」をbasic modelと呼称し，FDAでは最大血漿中阻害薬濃度（結合形＋非結合形）を使用して算出したR値が1.1より大きい場合に臨床薬物相互作用試験を考慮することを推奨している。本邦では，このR値をカットオフ基準と呼び，FDAと同様の基準（$R>1.1$）を採用した（EMAの基準「$R>1.02$，[I]は最大血漿中非結合形阻害薬濃度」とは異なる）。また，カットオフ基準に続く判断基準として設定したメカニズムに基づく静的薬物速度論（mechanistic static PK；MSPK）モデルは，FDA及びEMAと同一の基準であるAUC比>1.25（誘導の場合：AUC比<0.8）を採用した[7]。

2）欧米規制当局の指針との相違点

上述したカットオフ基準のほかに，欧米規制当局の指針との相違点について以下に触れる。

FDAでは，複数の代謝酵素の合算が全身クリアランスの25%以上を占めると予想される場合についても，相互作用を受ける可能性について検討することを推奨しているが，本邦においてはEMAと同様に単一酵素の寄与が25%以上を占める場合に限定した。また，FDAでは，被験薬がUGT基質であった場合については，別途，臨床薬物相互作用試験の実施に関する決定樹を提唱しているが，内因性基質であるビリルビンを除き，UGT阻害に基づく明確な臨床薬物相互作用の報告例がないことから，本邦においては*in vitro*試験による分子種推定と主要なUGT分子種（UGT1A1，UGT2B7など）に対する阻害作用の評価を推奨するまでにとどめた。

酵素誘導の指標としては，欧米の指針に合わせてmRNAの発現変動を推奨するが，被験薬が酵素阻害（特に時間依存的阻害）を有していない場合には，酵素活性を評価項目とすることも許容している。これは，mRNAを指標とした酵素誘導の定量的予測については，これまでのところCYP3Aを対象とした検証しかなされていないためである[8]。また，相互作用を受ける側としての臨床における酵素誘導試験は，対象となる代謝酵素の強い阻害薬を用いた臨床薬物相互作用試験（阻害試験）の結果から，シミュレーションなどにより臨床的に問題となる薬物相互作用が生じるリスクがあると判断された場合のみ必要とし，阻害薬と誘導薬を同列に扱っているFDAとは異なり，EMAの決定樹に類似した内容とした。

2-3　トランスポーターが関わる薬物相互作用の予測の考え方

近年の薬物動態制御因子としてのトランスポーターの重要性に関する知見が蓄積するにつれて，FDAおよびEMAが策定した薬物相互作用ガイダンス案・ガイドラインにおいては，薬物トランスポーターを介した薬物相互作用の予測に関する記載が大幅に増加している。FDAガイダンス案については2007年に，産官学のトランスポーターに関するエキスパートにより構成されたInternational Transporter Consortium（ITC）によって議論がなされたのち，2010年に“FDAトランスポーター白書”の位置づけとして発表さ

れた総説[9]の内容を概ね踏襲している。本項では，日本の新ガイドライン案におけるトランスポーターを介した相互作用予測の考え方，特にFDAとEMAとの相違点に焦点を絞り概説する。

1）対象とするトランスポーター群

現行のFDAガイダンス案においては，相互作用の観点から，新規化合物が基質・阻害薬になる可能性を検討すべきトランスポーターとして，主に小腸や腎臓・脳等，広範に発現する排出トランスポーターであるP-glycoprotein（P-gp），breast cancer resistance protein（BCRP），肝取り込みトランスポーターのorganic anion transporting polypeptide（OATP）1B1，1B3，腎取り込みトランスポーターのorganic cation transporter 2（OCT2），organic anion transporter（OAT）1と3が挙げられている[3]。一方，EMAのガイドラインには，上記のトランスポーターに加えて，カチオン類の肝取り込みに関わるOCT1，腎尿細管上皮細胞から尿側への排出に関わるmultidrug and toxin extrusion transporter（MATE）類（MATE1，MATE2-K）が記載されている[4]。OCT2については，FDAガイダンス案では，もともとcimetidineの相互作用点としての重要性から選択されている[3]が，一方，近年の研究により，ヒト臨床血中薬物濃度と阻害定数を考慮すると，腎排泄の阻害は，OCT2の阻害ではなくMATE類の阻害と考える方が妥当であるとする報告が複数でている[10-12]。そこで，日本のガイドライン案では，現行の薬物相互作用に関するヒト臨床での知見を考慮し，FDAが重視するトランスポーター7種類に加え，MATE類を検討すべきトランスポーターに追加した（MATE類の扱いについては，最近ITCより出された総説で，MATEの基質・阻害薬の判定に関する決定樹の試案がでている[13]ことから，FDAガイダンス案に今後追記される可能性が考えうるが定かではない）。一方で，第2回ITC workshopにおいて，今後重視すべき対象となるトランスポーターの候補として，ビリルビンのグルクロン酸抱合体を胆汁中へ排出輸送するmultidrug resistance-associated protein 2（MRP2），胆汁酸を胆汁中へ排出輸送するbile salt export pump（BSEP）が議論されている[14]が，これらの阻害が肝毒性に必ず直結するといったエビデンスが少ないことから，日本の案ではこれらは留意事項として，内因性基質と薬物の相互作用に関する注意を促すにとどめた。

2）P-gp，BCRPが関わる相互作用の検討

基質・阻害薬の評価においては，基本的にFDA法を踏襲した。基質としては，Caco-2やP-gp発現細胞における flux ratio（＝basal-to-apical flux/apical-to-basal flux）やnet flux ratio（＝発現細胞でのflux ratio/対照細胞でのflux ratio）が2以上で基質と判定する。阻害薬としては，循環血からの輸送阻害を考慮した$[I_1]/IC_{50}>0.1$（$[I_1]$＝阻害薬の循環血中最大総濃度，IC_{50}＝阻害薬による50%阻害濃度）もしくは，消化管内からの輸送阻害を考慮した$[I_2]/IC_{50}>10$（$[I_2]$＝投与量/250 mL）のいずれかを満たすとき，*in vivo*阻害薬と判定する。いずれの場合も臨床薬物相互作用試験を推奨する。ただし，BCRP基質の場合，現状で，臨床使用可能な適切なBCRP阻害薬がないことから臨床試験による実証は求めないが，一方で，日本人に比較的頻度が高い機能低下を引き起こす遺伝子多型（c.421C>A）が既知である[15]ことから，BCRP基質であることの情報提供は求めるという姿勢をとった。

3）OATP1B1，OATP1B3が関わる相互作用の検討

基質の判定については，FDAの決定樹とは2カ所異なっている。1つは，OATP1B1/B3の基質となるかを調べる試験を免除できるかを判定するところで，肝選択的な集積がないことを立証するために，動物オートラジオグラフィーの結果を利用できることを明確化した。また，基質の膜透過性の低さや中性域での電荷が陰性であることについては，OATP1B1/1B3のこれまでの基質の特性に鑑み，常に正しいとは限らないことから，先入観を排除するために決定樹の記載からは削除した。もう1つは，基質の判定において，遺伝子発現細胞以外にヒト肝細胞の利用も併記した。OATP1B1とOATP1B3の関与を分離できない弱点はあるが，現段階でヒト臨床において相互作用を引き起こす阻害薬が1B1/1B3選択性に乏しいことから[16]，相互作用の評価に限れば，実用上は当面問題ないと考えている。

一方，阻害薬の判定については，FDA法では，$C_{max}/IC_{50}>0.1$，かつ$1+I_{u,inlet,max}/IC_{50}>1.25$（$I_{u,inlet,max}$：門脈中最大非結合形薬物濃度）の基準を満たした場合，阻害薬とみなし，臨床相互作用試験を推奨している[3]が，日本版では1段階目の基準を削除して，2段階目のみの判定とした。その根拠としては，実際に相互作用が報告されている一部のOATP阻害薬において，1段階目の基準はnegativeと判定されるものの，2段階目ではpositiveと判定され，FDA法では，かえってfalse-negativeな判定につながる危険性があると判断したためである。一方，阻害薬の評価濃度の選択に当たっては，既知のOATP類を介すると想定される臨床相互作用事例について網羅的な解析を行った結果，$I_{u,inlet,max}$を用いた予測が最もfalse-negativeを避ける

ことができたこと[16]からも，妥当であると考えている。一方，EMA 法では，$1+I_{u,inlet,max}/IC_{50}>1.04$ であり[4]，かなり厳しい基準が設定されている。

4）OAT1，OAT3，OCT2，MATE1，MATE2-K が関わる相互作用の検討

基質の判定については，FDA の決定樹を踏襲している[3]が，MATE 類を新たに追記した。基質となった場合，前述の通り MATE 類については，cimetidine を阻害薬として用いた臨床薬物相互作用試験を推奨する一方，OCT2 の基質となった場合は，BCRP の時と同様に臨床で用いうる阻害薬が存在しないことから，情報提供にとどめるとの記載をした。一方，阻害薬の判定については，FDA 法では，$1+I_{u,max}/IC_{50}>1.1$[3]，EMA 法では，>1.02[4] をカットオフ値として用いているが，日本の案においては，AUC の 1.25 倍以上の上昇を判定することから，現時点で特段の配慮すべき臨床事例がないことも考慮して，$1+I_{u,max}/IC_{50}>1.25$ をカットオフ値と設定した。

2-4　添付文書における薬物相互作用に関する記載について

新医薬品の開発では薬物相互作用に関する検討が段階的に実施され，収集されたデータおよび注意喚起が添付文書などを通じて医療現場に提供される。医療用医薬品の添付文書は，医薬品の適正使用のための基本的な要約情報であり，記載要領は平成 9 年および平成 12 年の通知等[17,18]に基づく。添付文書での相互作用の注意喚起は，併用禁忌（併用しないこと）と併用注意（併用に注意すること）との措置分類に大別される。使用上の注意の「相互作用」において，表形式を基本として，薬剤名または薬効群名ごとに臨床症状・措置方法と機序・危険因子に分けて相互作用の内容と注意事項が記載され，関連データや相互作用試験の成績は「薬物動態」において情報提供される。

新ガイドライン案には，添付文書における相互作用の注意喚起と情報提供に関して，以下の内容を盛り込んだ。

① 措置分類は従来通りの 2 分類とし「相互作用」欄に記載する。加えて，重複記載を避けることを原則としつつ，生じ得る相互作用の臨床的な重要度に基づき，必要な場合にはリスク管理のための注意事項や投与指針を「相互作用」欄以外の使用上の注意の項目へも具体的に記載する。

② 薬物代謝酵素シトクロム P450 の各分子種の阻害薬，誘導薬，基質は，臨床相互作用データに基づいた強度分類を行い整理した。本分類は臨床相互作用試験で用いる指標薬の選択や添付文書での情報提供に活用できる。

③ 臨床相互作用試験の成績，症例報告又はモデリングによる相互作用予測など，エビデンスレベルの違いを考慮した適切な情報提供を行う。

④ 臨床相互作用試験はその結果にかかわらず，臨床的な影響の有無や試験成績について必要な情報を「薬物動態」において使用者側が理解しやすい形式にて提供する。

新ガイドラインに基づき，医薬品開発時の薬物相互作用の検討内容が適切に情報提供され，医療現場において適正な相互作用のリスク管理が行われることを期待したい。

③ おわりに

本稿では，新たな薬物相互作用ガイドラインの必要性，新ガイドラインの記載根拠となる薬物相互作用に関する科学的な知見，新ガイドラインにおける薬物相互作用評価とその添付文書への反映についての基本的な考え方を，主として薬物代謝およびトランスポーターの面から述べた。

新ガイドライン案は，全体として国際的な調和を保つ内容となっているが，その項目立ては現行の日本のガイドラインを踏襲するとともに，トランスポーターに関する最新知見や民族差に基づく遺伝子多型の記載など本邦のアカデミア研究の知見を基に若干記載が異なる部分もある。FDA や EMA 版にはない，一定の科学的エビデンスに基づいて選択された *in vivo*，*in vitro* 試験で推奨される典型的な基質や阻害薬の表を新たに作成した。また，紙面の都合上から割愛したが，臨床試験の必要性判断のための小腸における CYP3A 阻害のクライテリアは，いずれも極めて保守的に設定されており，消化管におけるトランスポーター阻害の影響を指標とした設定値を流用しているのが現状である[19]。これらを参考にして，円滑に相互作用の予測が進むことを願っている。なお，トランスポーターを介した臨床薬物相互作用は，まだまだ事例の集積が少なくエビデンスの蓄積とともに，相互作用の判断法についてもサイエンスの進歩とともに変化する可能性がある。

新ガイドラインは，平成 26 年度初旬の通知を目指している。これにより，臨床上問題となる薬物相互作用が発現する可能性を早期に判断することで，医薬品開発の効率化に資するとともに，開発時に得られた情報を適切に臨床現場に提供することにより，有害な薬物相互作用の発現や有効性の低下が回避され，医薬品のベネフィットとリスクのバランスを最適化し，適正使用が促進されることが期待される。また，迅速な医薬品開発に資するための国際的ハーモナイゼーションをよりいっそう推進し，各極の規制当局による指針

の相違点を解消するとともに，臨床試験の必要性判断のためのクライテリア設定を目的とした検証試験に産官学の研究者が一体となって取り組むことが望まれる。

参考文献

1）厚生労働省医薬局審査管理課長通知：「薬物相互作用の検討方法について」（平成13年6月4日，医薬審発第813号）
2）加藤陞一他，非臨床薬物動態試験・薬物相互作用ガイドライン検討班：「薬物相互作用の検討方法について」解説，医薬品の臨床薬物動態試験，83-123，じほう，2003
3）US Food and Drug Administration (FDA): Guidance for Industry, Drug Interaction Studies—Study Design, Data Analysis, Implications for Dosing, and Labeling Recommendations. Feb. 2012
4）European Medicine Agency (EMA): Guideline on the investigation of drug interactions. Jun. 2012
5）厚生労働省医薬食品局：医薬品開発と適正な情報提供のための薬物相互作用ガイドライン（案）http://www.nihs.go.jp/whlw/20131488.pdf
6）Ito K, Iwatsubo T, Kanamitsu S, Ueda K, Suzuki H, Sugiyama Y: Prediction of pharmacokinetic alterations caused by drug-drug interactions: metabolic interaction in the liver. Pharmacol Rev. 50, 387-412, 1998
7）Fahmi OA, Hurst S, Plowchalk D, Cook J, Guo F, Youdim K, Dickins M, Phipps A, Darekar A, Hyland R, Obach RS.: Comparison of different algorithms for predicting clinical drug-drug interactions, based on the use of CYP3A4 *in vitro* data: predictions of compounds as precipitants of interaction. Drug Metab Dispos. 37, 1658-1666, 2009
8）Fahmi OA, Kish M, Boldt S, Obach RS.: Cytochrome P450 3A4 mRNA is a more reliable marker than CYP3A4 activity for detecting pregnane X receptor-activated induction of drug metabolizing enzymes. Drug Metab Dispos, 38, 1605-1611, 2010
9）Giacomini KM, Huang SM, Tweedie DJ, Benet LZ, Brouwer KL, Chu X, et al.: Membrane transporters in drug development. Nat Rev Drug Discov, 9, 215-236, 2010
10）Ito S, Kusuhara H, Yokochi M, Toyoshima J, Inoue K, Yuasa H, et al.: Competitive inhibition of the luminal efflux by multidrug and toxin extrusions, but not basolateral uptake by organic cation transporter 2, is the likely mechanism underlying the pharmacokinetic drug-drug interactions caused by cimetidine in the kidney. J Pharmacol Exp Ther, 340, 393-403, 2012
11）Matsushima S, Maeda K, Inoue K, Ohta KY, Yuasa H, Kondo T, et al.: The inhibition of human multidrug and toxin extrusion 1 is involved in the drug-drug interaction caused by cimetidine. Drug Metab Dispos, 37, 555-559, 2009

12）Tsuda M, Terada T, Ueba M, Sato T, Masuda S, Katsura T, et al.: Involvement of human multidrug and toxin extrusion 1 in the drug interaction between cimetidine and metformin in renal epithelial cells. J Pharmacol Exp Ther, 329, 185-191, 2009
13）Hillgren KM, Keppler D, Zur AA, Giacomini KM, Stieger B, Cass CE, et al.: Emerging transporters of clinical importance: an update from the International Transporter Consortium. Clin Pharmacol Ther, 94, 52-63, 2013
14）Zamek-Gliszczynski MJ, Hoffmaster KA, Tweedie DJ, Giacomini KM, Hillgren KM.: Highlights from the International Transporter Consortium second workshop. Clin Pharmacol Ther, 92, 553-556, 2012
15）Ieiri I.: Functional significance of genetic polymorphisms in P-glycoprotein (MDR1, ABCB1) and breast cancer resistance protein (BCRP, ABCG2). Drug Metab Pharmacokinet, 27, 85-105, 2012
16）Yoshida K, Maeda K, Sugiyama Y.: Transporter-mediated drug--drug interactions involving OATP substrates: predictions based on *in vitro* inhibition studies. Clin Pharmacol Ther, 91, 1053-1064, 2012
17）厚生省薬務局長通知：「医療用医薬品添付文書の記載要領について」（平成9年4月25日，薬発第606号），「医療用医薬品の使用上の注意記載要領について」（平成9年4月25日，薬発第607号）
18）厚生省薬務局安全課長通知：「医療用医薬品添付文書の記載要領について」（平成9年4月25日，薬安第59号），厚生省医薬安全局安全対策課事務連絡：「医療用医薬品の使用上の注意の記載について」（平成12年12月25日）
19）Zhang L, Zhang Y, Strong JM, Reynolds K, Huang S-M.: A regulatory viewpoint on transporter-based drug interactions. Xenobiotica, 38, 709-724, 2008

（伊藤 清美，大野 泰雄，久米 俊行，斎藤 嘉朗，鈴木 洋史，永井 尚美，樋坂 章博，前田 和哉）